Ingeniería Investigación y Tecnología
volumen XIX (número 1), enero-marzo 2018 113-123
ISSN 2594-0732 FI-UNAM artículo arbitrado
Información del artículo: 25 de enero de 2017, reevaluado: 25 de abril de 2017, aceptado: 12 de julio de 2017

DOI: http://dx.doi.org/10.22201/fi.25940732e.2018.19n1.010

Synthesis and characterization of a polymeric magnetic hybrid material composed of iron oxide nanoparticles and polyvinyl butyral

Síntesis y caracterización de un material polimérico híbrido magnético de nanopartículas de óxido de hierro en una matriz de polivinil butiral

Reyes-Melo Martín Edgar
Universidad Autónoma de Nuevo León
E-mail: edgar.reyesml@uanl.edu.mx

Torres-Castro Alejandro
Universidad Autónoma de Nuevo León
E-mail: alejandro.torrescs@uanl.edu.mx

Puente-Córdova Jesús Gabino
Universidad Autónoma de Nuevo León
E-mail: jesus_ime@hotmail.com

García-Loera Antonio Francisco
Universidad Autónoma de Nuevo León
E-mail: antonio.garcial@uanl.mx

López-Walle Beatriz
Universidad Autónoma de Nuevo León
E-mail: beatriz.lopezwl@uanl.edu.mx

Abstract

A *Polymeric Magnetic Hybrid Material* (PMHM), consisting of iron-oxide nanoparticles synthesized in-situ in a *Polymer Matrix of Polyvinyl Butyral* (PVB), was developed in two stages. First, a precursor film hybrid material (Fe(II)-PVB) was obtained. In the second stage, Fe(II)-PVB was treated with H_2O_2 under alkaline conditions to obtain the PMHM. Characterization by XRD shows that the crystalline structure of iron oxide into PMHM corresponds to goethite, and to maghemite or magnetite phases. FTIR-spectroscopy reveal that the PVB-matrix preserves its chemical structure into the PMHM. HRTEM-images show that iron oxide nanoparticles (~5 nm) with sphere-like morphology are embedded into PVB-matrix; and diagrams of magnetization versus temperature, show that embedded nanoparticles have a superparamagnetic-like behavior. Finally, magnetorheological results show that mechanical properties of PMHM can be modified under the application of an external magnetic field, showing that it is a good alternative to carry out functions as actuator or sensor in electronic or mechatronic devices.
Keywords: magnetic properties, hybrid material, polymer, nanoparticles, iron oxide.

Resumen

Se desarrolló un proceso de síntesis en dos etapas para la obtención de un material híbrido magnético (PMHM) con matriz polimérica, el cual se compone de nanopartículas de óxido de hierro sintetizadas in-situ en una matriz de polivinil butiral o PVB. En la primera etapa, se sintetizó un material precursor en forma de película (Fe(II)-PVB). En la segunda etapa, el Fe(II)-PVB se trató con H_2O_2 bajo condiciones alcalinas para la obtención del PMHM. Mediante caracterización de difracción de rayos X o DRX se demostró que la estructura cristalina del óxido de hierro en el PMHM corresponde a fases de goethita y de maghemita o magnetita. Mediante espectroscopia FTIR se identificó que la matriz polimérica o PVB del PMHM conserva su estructura química. Imágenes obtenidas mediante HRTEM muestran que las nanopartículas de óxido de hierro (~ 5 nm) tienen formas cuasi-esféricas y están embebidas en la matriz de PVB. Por otra parte, los diagramas de magnetización versus temperatura, muestran que las nanopartículas en el PVB tienen un comportamiento superparamagnético. Finalmente, los resultados magnetoreológicos muestran que las propiedades viscoelásticas del PMHM pueden modificarse bajo la aplicación de un campo magnético externo, demostrando que es una buena alternativa para llevar a cabo funciones como actuador o sensor para el diseño de dispositivos electrónicos o mecatrónicos.
Descriptores: propiedades magnéticas, material híbrido, polímero, nanopartículas, óxido de hierro.

DOI: http://dx.doi.org/10.22201/fi.25940732e.2018.19n1.010

Introduction

A *Polymeric Magnetic Hybrid Material* or PMHM is a combination, at the nanoscale, of a magnetic-inorganic component and a polymeric matrix. In this kind of hybrid materials, the addition of a second phase at nanometric scale into a polymer matrix produce a synergy between constituents, such that new properties capable of meeting or exceeding design expectations can be achieved (Luna *et al*., 2013; Abellán *et al*., 2015). In this sense, the combination of the magnetic properties of iron oxide nanoparticles with the viscoelastic properties of a polymer matrix of polyvinyl butyral, PVB, is of great interest to carry out functions as actuators or sensors in electronic or mechatronic devices. These important applications are based in the fact that a PMHM-film has instant reaction and contactless control, because it responds to an external magnetic field. Additional applications could also be obtained for PMHM-films in considering that magnetic nanoparticles are very important due to their potential integration in a broad range of technological applications, extending from magnetic fluids (Jiang *et al*., 2014; Goncalves *et al*., 2015), catalysis (Jiang *et al*., 2014; Tan *et al*., 2015), ultrahigh-density magnetic storage media (Jiang *et al*., 2014; Galloway *et al*., 2015), biotechnology and biomedicine (Jiang *et al*., 2014; Wul *et al*., 2015a), and magnetic resonance imaging (Jiang *et al*., 2014; Shin *et al*., 2015). Nowadays, several kinds of magnetic nanoparticles can be synthetized, but metal oxides are preferred over pure metals nanoparticles because they are more stable to oxidation processes (Lu *et al*., 2007; Zhang *et al*., 2015a).

Concerning the polymer matrix component, it stabilizes the magnetic nanoparticles and offers both swelling ability and entropic elasticity to the PMHM films. In PMHM-films, nanoparticles are stabilized because polymer matrix endows the nanoparticles with functional groups necessary for the desired applications. The polymer matrix used in this work, PVB, is a polyacetal synthetized by reacting polyvinyl alcohol with butyraldehyde in acid medium (Zhou *et al*., 1997; Reyes *et al*., 2015; Xi and Zhi, 2016). Substantial amounts of unreacted vinyl alcohol units typically remain in the chain and so PVB is best regarded as a random copolymer of vinyl butyral and vinyl alcohol units. Figure 1 shows both the chemical structure of a segment of PVB-chain, and the relative proportions of alcohols or hydroxyl groups (B), acetate groups (C) and butyral groups (A). The proportions between A, B and C structural parameters are controlled by the conditions of the acetal reaction.

From the chemical structure of PVB, it is important to remark that the vinyl alcohol unit is polar and hydrophilic; and the vinyl butyral unit is hydrophobic. On the other hand, the hydroxyl and acetate groups act as promoters of polymer adhesives onto glass surfaces and other materials, such as metals and wood. In addition, PVB is a polymer with outstanding mechanical properties and excellent optical clarity. For these reasons, the main industrial application of PVB is in manufacture process of safety glass laminates, particularly in automotive and architectural glass (Reyes *et al*., 2015; Xi and Zhi, 2016; Fors, 2014; Zhang *et al*., 2015b)

This paper is focused on the synthesis and characterization of a PMHM composed of iron oxide nanoparticles and a polymer matrix of PVB. The main feature of PMHM is that its viscoelastic properties can be modified under action of a magnetic external field, showing that it is a good alternative to carry out the functions of actuators or sensors in electronic or mechatronic devices. In the next section the magnetic behavior of iron oxide nanoparticles are summarized.

Iron oxide nanoparticles

Iron oxide exists in many forms in nature, like magnetite (Fe_3O_4), maghemite (γ-Fe_2O_3), and/or hematite (α-Fe_2O_3) (Teja and Kho, 2009). Hematite is extremely stable at ambient conditions, and is the end product of the transformation of other phases of iron oxides. Magnetite exhibits the strongest magnetism of any transition metal oxide. Maghemite occurs in soils as a product of heating of other iron oxides, it is metastable with respect to hematite, and forms continuous solid solutions with magnetite (Teja and Kho, 2009; Wul *et al*., 2015b).

The iron with an oxidation state Fe^{2+} has a strong magnetic moment due to four unpaired electrons in its 3*d* orbitals. However, crystals that include Fe-ions can display different magnetic states: paramagnetic, ferromagnetic, antiferromagnetic, and ferrimagnetic. In paramagnetic state, the individual ion magnetic moments are randomly aligned with respect to each other, and the crystal has a zero net magnetic moment. If this crys-

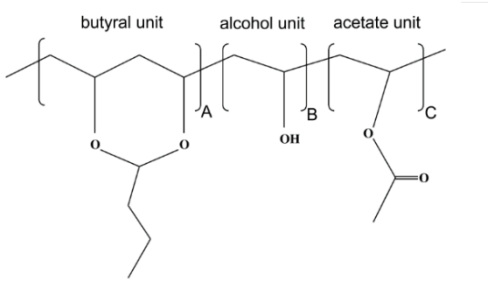

Figure 1. Chemical structure of a segment of PVB-chain

DOI: http://dx.doi.org/10.22201/fi.25940732e.2018.19n1.010

tal is subjected to an external magnetic field, $\vec{H}$, some of these moments will align, and the crystal will attain a resultant magnetic moment. On the other hand, in a ferromagnetic crystal, all the individual magnetic moments are aligned even without $\vec{H}$. In the case of ferrimagnetic crystals, they have a net magnetic moment from two types of atoms with moments of different strengths that are arranged in an antiparallel fashion. If the antiparallel magnetic moments have the same magnitude, then the crystal is antiferromagnetic and possesses no net magnetic moment. Because of the different magnetic states that the crystal structure of Fe-ions could display, the magnetic behavior for bulk iron oxide must be identified, and it can be characterized, by a magnetization vector, $\vec{M}$, that is the vector sum of all the magnetic moments of the ions in the material per unit volume. The magnitude of $\vec{M}$ is generally less than its value when all atomic moments are perfectly aligned, because the bulk material consists of domains with each domain having its own magnetization vector arising from an alignment of atomic magnetic moments within the domain. Because to the magnetization vectors of all the domains in the material may not be aligned, leading to a decrease in the overall magnetization, an important aspect is the fact that when the length scale of the material becomes small, the number of domains decreases until there is a single domain when the characteristic size of material is below some critical size d_c. In consequence, small particles at nanometer scale possess a single domain structure, consisting of groups of spins all pointing in the same direction and acting cooperatively (Jiang *et al*., 2014; Wul *et al*., 2015b). By contrast, larger particles (above 100 nm) possess multi-domain structures consisting of many single domains separated by domain walls, which produce magnetic flux closures rendering the bulk material macroscopically as non-magnetic (Teja and Kho, 2009). If an external magnetic field, $\vec{H}$, is applied to a ferromagnet of magnetic strength $|\vec{M}|$, a magnetization curve can be obtained showing that $|\vec{M}|$ increases with $|\vec{H}|$ until a saturation value $|\vec{M}_s|$ is reached. Then, the magnetization curve displays a hysteresis loop, because all domains do not return to their original orientations when $|\vec{H}|$ is decreased after the saturation magnetization value is attained. Thus, when $|\vec{H}|$ returns to zero, there is a remnant magnetization $|\vec{M}_r|$ which can only be removed by applying a coercive field $\vec{H}_c$ in the opposite direction to $\vec{H}$.

A single domain magnetic material has no hysteresis loop and is said to be superparamagnetic. In consequence, for the case of iron oxide nanoparticles smaller than about 20 nm often display superparamagnetic behavior at room temperature (Wul *et al*., 2015b). The dispersion of the superparamagnetic behavior of iron oxide nanoparticles into a PVB-matrix is the central idea in this work to obtain a PMHM. The industrial importance, which could have this material, is based on the fact that a PMHM-film must be able to deform in a controlled way, when a magnetic field is applied.

Experimental

Materials

Polyvinyl butyral S-Lec (PVB) with an average molecular weight of 53,000 *g/mol* was used in this work, it was supplied by Sekisui, Japan. As precursor salt of Fe^{+2}, ferrous chloride tetrahydrate ($FeCl_2 \bullet 4H_2O$, 99%) was used, it was supplied by Sigma-Aldrich. Sodium hydroxide (NaOH, 97%) supplied by Fermont was used to obtain alkaline conditions. Tetrahydrofuran (THF) supplied by Fisher Scientific was used as solvent. Finally, the hydrogen peroxide (H_2O_2, 3%) used was supplied by Zuum (Mexico City, Mexico). All materials were used as-received for the synthesis of the PMHM.

Synthesis of the polymeric magnetic hybrid material (PMHM)

The process to obtain the PMHM was performed in two stages. In the first one, it was synthesized a precursor film hybrid material, Fe(II)-PVB. In the second stage, the precursor material was used to synthesize iron oxide nanoparticles into PVB matrix. Both stages are described in this section.

Stage 1: 1.6 g of PVB was dissolved into 20 mL of THF, and then the PVB-THF obtained was stirred for 60 minutes (solution 1) at 40°C. On the other hand, a solution of 15 mL 0.268 M $FeCl_2 \bullet 4H_2O$ using THF as solvent was prepared (solution 2). Solutions 1 and 2 were mixed and stirred for 60 minutes. With the mixture ready, the precursor material is prepared by casting, at room temperature for 24 h, in order to eliminate the solvent by a natural convection process. After that, precursor film hybrid material (Fe(II)-PVB) was obtained. The thickness of the resulting film was measured using a Mitutoyo micrometer, the result obtained was ~20 μm.

Stage 2: In this experimental part, the precursor film hybrid material was submerged in an aqueous solution of 3.3 M NaOH at 50°C, obtaining a rapid change in color, from yellow to black. After that, 30 mL of H_2O_2

DOI: http://dx.doi.org/10.22201/fi.25940732e.2018.19n1.010

was added to the ''black material'' observing a color change from dark to brownish. Finally, the brownish material was washed several times with deionized water (18 MΩ-cm) to eliminate the residual products (NaOH and Cl^-). After that the PMHM was obtained.

Characterization of precursor material and PMHM

Both the precursor film hybrid material (Fe(II)-PVB) and the PMHM were studied by X-ray diffraction (XRD) to determine their crystallinity, by Fourier transform infrared spectroscopy (FTIR) to determine the vibration modes of chemical groups of the polymer matrix, by high-resolution transmission electron microscopy (HRTEM) to determine the structure and morphology of PMHM, by vibrating sample magnetometry (VSM) to determine the magnetic behavior of PMHM, and by magnetorheology analysis (MRA) to determine the effect of external magnetic field on the viscoelastic properties of PMHM.

The XRD measurements were carried out using a diffractometer Bruker D8 Advance, over the range from 20 to 80 degrees (2θ); three samples (PVB, Fe(II)-PVB and PMHM) were pulverized to perform X-ray diffraction analysis. The FTIR spectra were obtained using a FTIR spectrometer, IRAffinity Shimadzu, in transmittance mode, scanning 30 times at 2 cm^{-1} resolution from 400 to 4000 cm^{-1}. For this case, three samples (PVB, Fe(II)-PVB and PMHM) were used as thin films.

The structure and morphology of PMHM was studied by HRTEM. The analysis of transmission electron microscopy was done in a Titan FEI. The specimen was prepared by dispersing the PMHM powder in water using an ultrasonic bath and placing an aliquot of the dispersion onto a cooper TEM grid.

Magnetic properties were measured by VSM at room and low temperature (300 K and 4.2 K, respectively) using a quantum design SQUID-VSM magnetometer. A PMHM-specimen in the form of thin film was used for its analysis.

Finally, the effect of iron oxide nanoparticles on the rheology behavior of PMHM was analyzed by MRA. A film with a thickness of 20 μm was submitted to an oscillatory rheometry test between two parallel plates using an Anton Paar Rheometer MCR301 equipped with a magnetorheological device MRD 70-1T. The oscillating test was developed at room temperature (25°C) applying a constant magnetic field (~11 kOe) and applying a shear strain amplitude of 0.1% in a frequency interval from 0.01 to 100 Hz. The storage modulus (G') and the loss factor (tan δ) were registered.

Results and discussion

Characterization of the precursor film hybrid material (Fe(II)-PVB)

The microstructure of the precursor film hybrid material (Fe(II)-PVB) was studied by XRD and FTIR analysis. Figure 2a shows the X-ray pattern obtained for the PVB-sample. A broad band is observed at low 2θ values (lower than 50°), which is a typical result for amorphous polymers. Figure 2b shows the diffraction pattern obtained for the Fe(II)-PVB sample. This diagram shows a clear peak that correspond to a peak diffraction associated to iron hydroxides. This peak displayed at 27° is related with goethite phase (α-FeOOH), (Luna *et al*., 2013; Marinho, 2014), which was formed because of the tendency of the THF to form peroxides (Clark, 2001; Kumar and Singh, 2014) that produce oxidation process of Fe^{2+}. This diagram (Figure 2b) does not show peaks associated to the $FeCl_2 \bullet 4H_2O$ (see Figure 2c). Matching between Figures 2a, 2b and 2c suggest that $FeCl_2 \bullet 4H_2O$ was partially dissolved and partially oxidized into PVB matrix.

With respect to the FTIR analysis, the comparison between the FTIR-spectra for PVB and Fe(II)-PVB specimens, allows us to identify if the vibration modes of the chemical groups of the PVB are modified or not due to the presence of Fe^{2+} into the Fe(II)-PVB. Figure 3 shows the FTIR spectrum of a PVB sample, typical bands corresponding to PVB were identified; the broad band at 3486 cm^{-1} corresponds to the OH stretching modes; the band at 1739 cm^{-1} was attributed to the C=O stretching vibration of the acetate groups, the bands at 2871 cm^{-1} and 2956 cm^{-1} corresponded to symmetrical and asymmetrical stretching modes of CH_3 and CH_2, respectively; an absorption band corresponding to the C-O-C group of the cyclic acetal at 1130 cm^{-1} also is observed, finally another absorption band associated to group C-OH also is observed at 994 cm^{-1}. These results are in according with results obtained by El-Din *et al*. (1995).

Figure 4 shows a matching between the FTIR spectra of PVB, Fe(II)-PVB and the PMHM. Matching between PVB and Fe(II)-PVB samples shown that the vibration modes of chemical groups CH_2, CH_3, C=O, C-OH and C-O-C do not show significant shifts. This behavior is a consequence that precursor salt ions do not interact with these chemical groups in a major way. On the contrary, the vibration modes corresponding to OH groups are affected when the precursor salt (solution 2) is added to PVB (solution 1) to obtain the precursor film hybrid material (Fe(II)-PVB); consequently, bands associated to those chemical groups have a shift

DOI: http://dx.doi.org/10.22201/fi.25940732e.2018.19n1.010

towards lower wave numbers. This effect corroborates that OH-groups form with Fe^{2+} on the one hand iron hydroxides (α-FeOOH), (Marinho, 2014) and on the other hand Fe^{2+}-ions are coordinated with OH groups of the PVB-matrix (Luna *et al*., 2013). Table 1 resume the results obtained from FTIR analysis for the three samples studied.

Results obtained by XRD and FTIR analysis corroborate that $FeCl_2 \bullet 4H_2O$ was partially dissolved and partially oxidized into the PVB matrix. Figures 4a and 4c corresponding to PVB and PMHM samples are matched in next section.

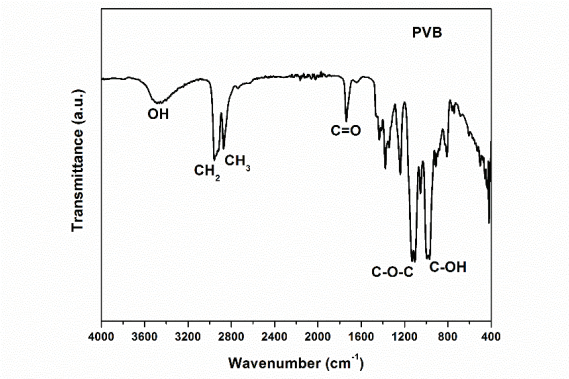

Figure 3. FTIR spectrum of PVB

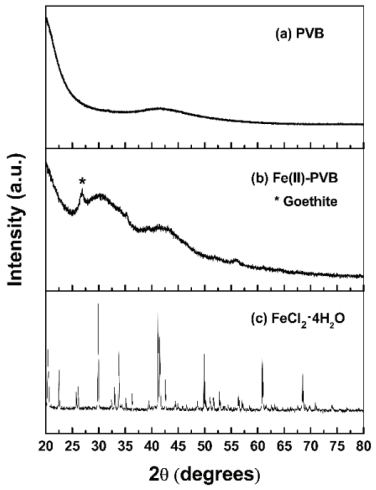

Figure 2. X-ray patterns for a) PVB-sample, and for b) precursor hybrid material Fe(II)-PVB, c) $FeCl_2 \bullet 4H_2O$

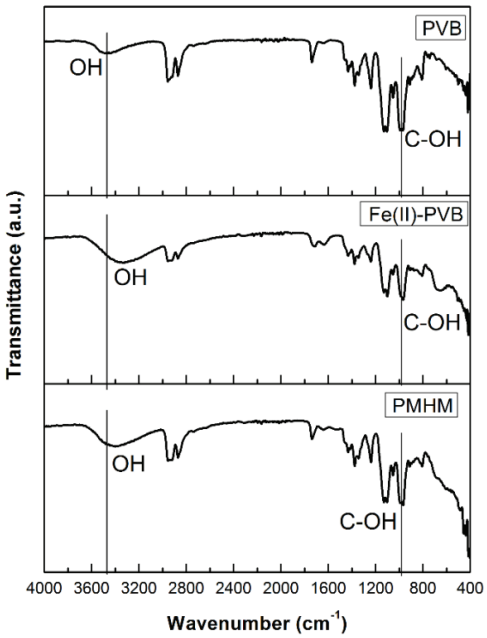

Figure 4. Matching between FTIR-spectrum of PVB, Fe(II)-PVB and PMHM

Table 1. FTIR results for the three samples: PVB, Fe(II)-PVB and PMHM

Assignments	Wavenumber (cm^{-1})		
	PVB	Fe(II)-PVB	PMHM
C-OH, stretching	994	968	968
C-O-C, symmetric stretching	1130	1129	1129
C=O, stretching	1739	1714	1738
CH_3, CH_2, symmetric and asymmetric stretching	2871.2956	2871.2956	2870.2955
OH, stretching	3486	3336	3399

DOI: http://dx.doi.org/10.22201/fi.25940732e.2018.19n1.010

Characterization of the PMHM

After chemical treatment (stage 2) of the Fe(II)-PVB with H_2O_2 under alkaline conditions, its change in color was from black to brownish, this fact suggests the formation of iron-oxide nanoparticles embedded into the PVB matrix. To corroborate this fact, ''brownish material'' was studied by XRD analysis. Figure 5a shows the diffraction pattern obtained. A peak (*) associated to goethite phase is observed, and another diffraction peaks are identified at 30.26°, 35.34°, 39.37°, 53.82°, 56.27°, and 62.54° that correspond to the (220), (311), (320), (422), (511) and (440) plane reflections of maghemite (Figure 5b) or magnetite (Figure 5c) crystalline structures (Luna *et al*., 2013; Jiang *et al*., 2014; Wul *et al*., 2015b; ICDD, 2000a and b).

On the other hand, the interaction between iron oxide nanoparticles and PVB-matrix was studied by FTIR analysis. Figure 4 corresponds to the matching between FTIR spectra of PVB and PMHM samples. With the exception of the vibration modes of OH groups, practically all the other bands corresponding to PVB do not suffer any shift; this means that the synthesized iron oxide nanoparticles interact with the PVB through its OH groups (see Table 1). This fact is very important because it is through the interface between the iron oxide nanoparticles and the polymer matrix that the effect of the body force of an applied magnetic field must be transmitted from nanoparticles to the polymer matrix, generating a surface force that induces the deformation into the PMHM (Aowlad *et al*., 2012; Philippova *et al*., 2011).

The size and morphology of iron oxide nanoparticles into PMHM were studied by HRTEM analysis. The

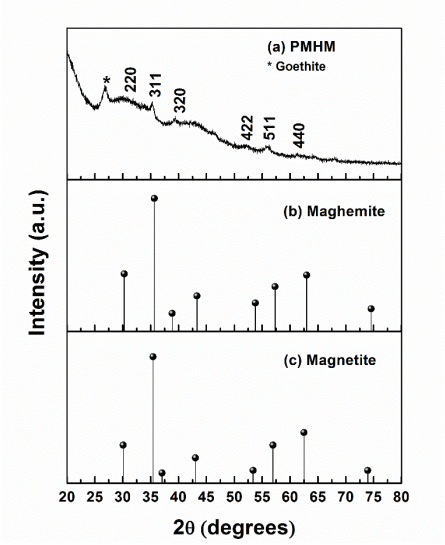

Figure 5. a) Diffraction peaks corresponding to PMHM, b) maghemite and c) magnetite standards

HRTEM images (Figure 6a) show a higher number of iron oxide nanoparticles with sphere-like morphology. Regions corresponding to these nanoparticles were analyzed by energy dispersed spectroscopy (EDAX), and results reveals an elemental composition of Fe 5.15 atm.%, C 69.15 atm.%, O 24.43 atm.% and Na 1.26 atm.%. The average particle size of the iron oxide nanoparticles was measured from different HRTEM-images using image analysis (Digital Micrograph Software of Gatan), and the frequency histogram shows an average size of 5 nm (Figure 6b). These results suggest that the magnetic behavior of the nanoparticles obtained must be superparamagnetic, because according to the literature, the number of magnetic domains decreases until there is a single domain when the characteristic size of material is below some critical size, in consequence small particles at nanometer scale possess a single magnetic domain, consisting of groups of spins all pointing in the same direction and acting cooperatively, and the magnetic behavior produced for these nanoparticles are labeled as superparamagnetic (Zhang *et al*., 2015b; Teja and Koh, 2009; Sommertune *et al*., 2015). This phenomena was corroborated by magnetization measurements and the result obtained are shown in Figure 8.

The HRTEM images of the iron-oxide nanoparticles are shown in Figures 7a and 7b. The well-defined lattice fringes correspond to crystallographic planes of iron oxide nanoparticles and they are identified in both figures.

From these HRTEM images, and using a Gatan Microscopy Suite Software (Version 2.0.1), the interplanar distances of 0.37, 0.29, and 0.23 nm were computed. These computed values correspond to interplanar distances of (210), (220), and (320) planes (Jiang *et al*., 2014; ICDD, 2000a and b). These crystallographic planes are of maghemite crystalline structure, which is consistent with the XRD analysis. The interplanar distances are very close to the computed values, shown in Table 2.

The magnetic behavior of the PMHM was studied by magnetization measurements. Figure 8 shows the magnetization curve at room temperature (300 K). The saturation magnetization value $|\overrightarrow{M_s}|$ is higher than 0.2 emu/cm^{-3} (0.638 emu/g Fe_2O_3) whereas both, remnant magnetization, $|\overrightarrow{M_r}|$ and coercitivity, $|\overrightarrow{H_c}|$, are undetectable. These last results corroborate the superparamagnetic behavior of the PMHM, because for a superparamagnetic behavior their magnetization curves not display a hysteresis loop (Teja and Koh, 2009; Philippova *et al*., 2011; Sommertune *et al*., 2015).

On the other hand, Figure 9 presents the magnetization curve at 4.2 K, and both coercive field and remnant magnetization values are different to zero. It can be

DOI: http://dx.doi.org/10.22201/fi.25940732e.2018.19n1.010

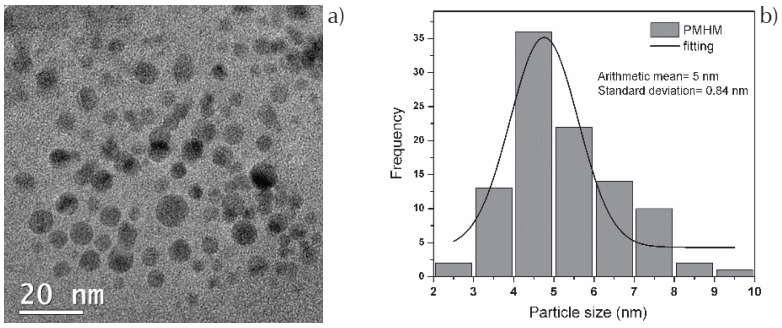

Figure 6. a) HRTEM-image of PMHM, b) particle size distribution

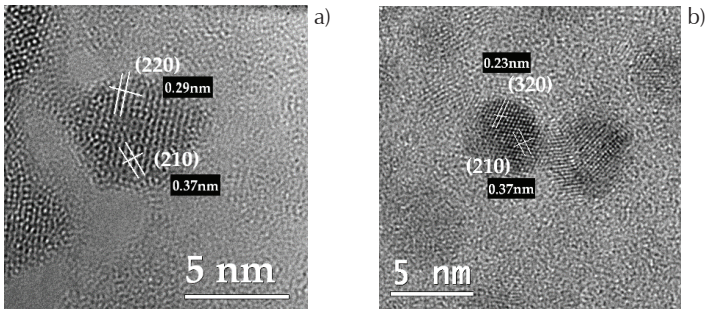

Figure 7. a) and b) HRTEM images in two different regions

Table 2. Summary data for calculated d [d(exp)] spacing from experimental X-ray patterns [2θ (exp)] and from ICDD-data base for iron oxide [d(γ-Fe_2O_3)], [d(Fe_3O_4)], and Miller indices, respectively (ICDD, 2000a and b)

hkl	*d*(computed)	*d*(γ-Fe_2O_3)	*d*(Fe_3O_4)
220	0.2953	0.2953	0.2967
311	0.2539	0.2517	0.2532
320	0.2288	0.2316	-
422	0.1703	0.1704	0.1714
511	0.1634	0.1607	0.1615
440	0.1485	0.1475	0.1484

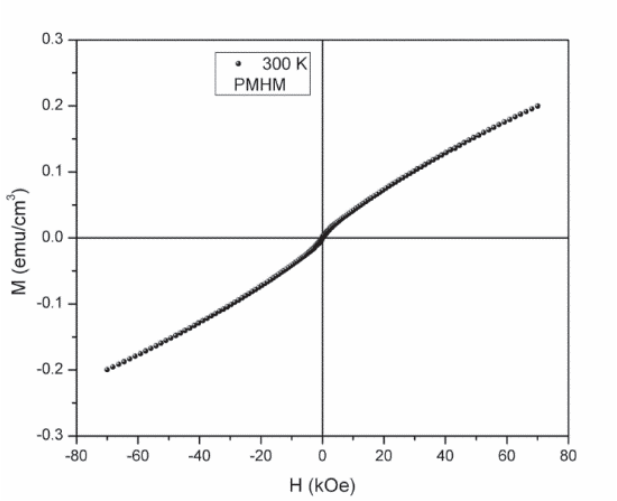

Figure 8. Magnetization curve of PMHM at 300 K

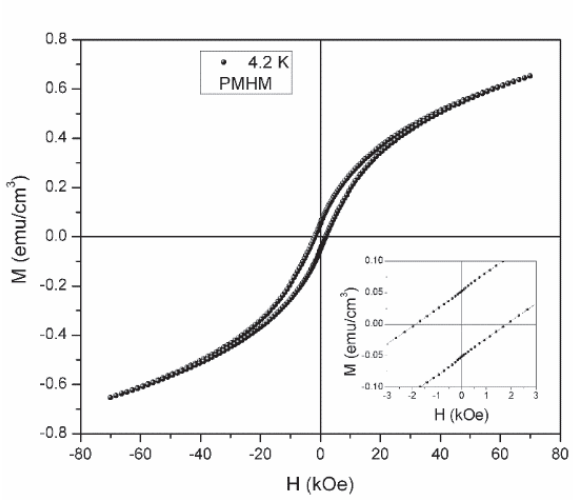

Figure 9. Magnetization curve of PMHM at 4.2K

DOI: http://dx.doi.org/10.22201/fi.25940732e.2018.19n1.010

seen that the corresponding values for the different magnetic parameters are 0.65 emu/cm^3 (2.075 emu/g Fe_2O_3) for saturation magnetization, $|\overrightarrow{M_s}|$, 1.81 kOe for coercive field, $|\overrightarrow{H_c}|$, and 0.05 emu/cm^3 (0.16 emu/g Fe_2O_3) for remanence value, $|\overrightarrow{M_r}|$ (inset Figure 9). Magnetization curves of Figure 9 correspond to a ferromagnetic behavior, and it is well known that it appears when the magnetic analysis is performed below the blocking temperature, T_B (Philippova *et al*., 2011; Sommertune *et al*., 2015; Kucheryavy *et al*., 2013).

To estimate T_B, for the PMHM sample, field-cooled (FC) and zero-field cooled (ZFC) analyses (Luna *et al*., 2013; Joy *et al*., 1998) were performed at a magnetic field of 100 Oe (Figure 10). When the PMHM sample is cooled at zero magnetic field (ZFC), Figure 10 shows that the total magnetization is small, but not zero (it is 43% of the maximum), as the magnetic particles are not fully random. When temperature increases, the nanoparticle magnetic moment is oriented with the external field increasing the total magnetization until it reaches a maximum at 25 K which is the value of the T_B. At this temperature, the thermal energy becomes comparable to the energy gained by aligning the nanoparticle magnetic vector in the weak field. At this point, the transition from ferromagnetic to superparamagnetic behavior is observed (Joy *et al*., 1998; Torres *et al*., 2014). When all nanoparticles are at the superparamagnetic relaxation state, above T_B, their magnetization follows Curie's law decreasing with increasing temperature. In the case of FC, magnetization monotonically increases as the temperature decreases because the nanoparticles are cooled from room temperature under a magnetic field and the magnetization direction of all the nanoparticles is frozen in the field direction (Joy *et al*., 1998). The magnetization shows the maximum at 4.2 K in the FC process (Figure 10). These result shown that iron oxides nanoparticles embedded into PVB matrix, respond with a superparamagnetic behavior to a magnetic field stimulus, and the superparamagnetic response must be transmitted to polymer matrix trough the interface nanoparticle-polymer, where OH groups plays and important roll.

Finally, to test the effect of an external magnetic field onto viscoelastic properties of the PMHM, magnetorheological behavior was analyzed, with and without external magnetic field. For the case of the test without external magnetic field, a film of PMHM with a thickness of 20 μm was tested with a sinusoidal strain stimulus, and the response, a sinusoidal stress, was registered for several frequencies from 0.1 to 100 Hz. For the case of the test with external magnetic field, a constant magnetic field of 11 kOe was applied and using the previous protocol. For the two analysis (with and without external field), from the applied stimulus and the registered responses, the complex modulus as a function of frequency was computed, $G^* = G' + iG''$. The real part, G', is associated to stored energy and represents the elastic behavior of the PMHM. On the other hand, the imaginary part, G'', is related to dissipated energy a represents the viscous behavior of the PMHM. From G' and G'' data, the relationship between the stored energy and dissipated energy also known as loss factor was computed, this parameter is represented by $\tan\delta = G''/G'$ (Reyes *et al*., 2004; Hebert *et al*., 2008). For polymeric material, typically, G' and $\tan\delta$ are used to determine the viscoelastic behavior of the samples studied. Typical rheological curves of G' and $\tan\delta$ were obtained (Figures 11 and 12) for the PMHM samples, in both cases when frequency increases, G' also increases and on the other hand $\tan\delta$ decreases. However, when the exter-

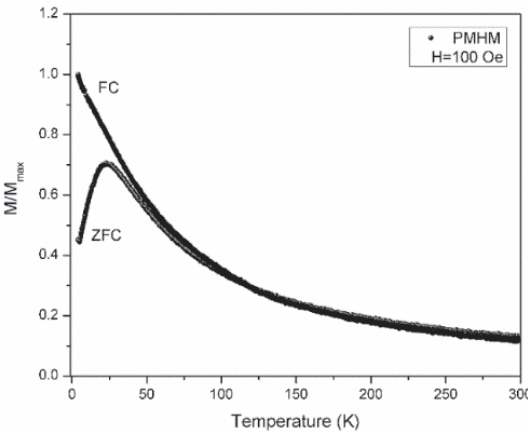

Figure 10. ZFC and FC magnetization curves at 100 Oe

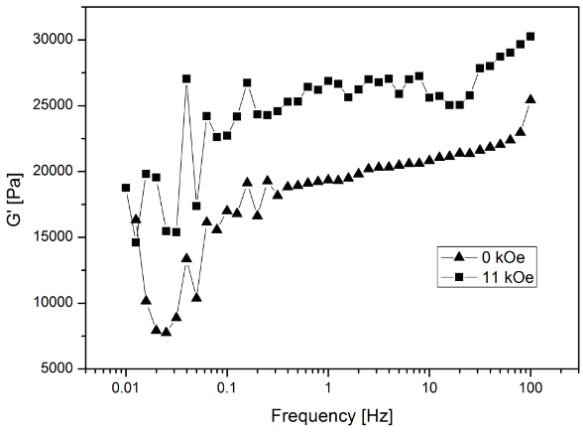

Figure 11. Magnetorheology measurements of PMHM, G' vs frequency

DOI: http://dx.doi.org/10.22201/fi.25940732e.2018.19n1.010

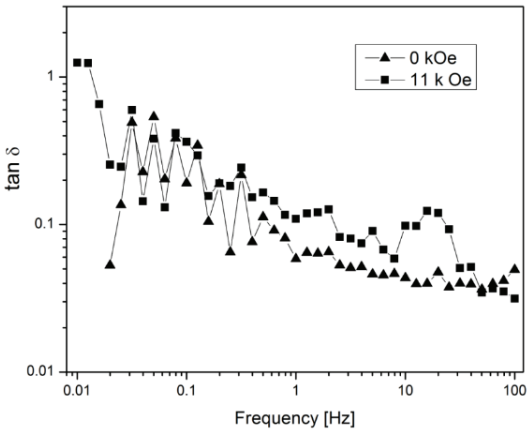

Figure 12. Magnetorheology measurements of PMHM, *tan* δ vs frequency

nal magnetic field (11 kOe) is applied, rheological curves are modified. Figure 11 show the effect of 11 kOe of external magnetic field on to *G´*. A global increases of *G´* is observed when magnetic field is applied. In other words, its capacity to store mechanical energy increases when the external magnetic field is applied. This is presumably due to the interactions between iron oxide nanoparticles and the polymer matrix (PVB). Finally, Figure 12 shows that tan δ do not increases in a very important way, this means that the capacity of the PMHM to dissipate energy (associate to *G´´*) increases in a similar way to increasing the capacity to store energy (associate to *G´*).

These latest results, Figures 11 and 12, show that the viscoelastic properties of the PMHM can be modified under action of a magnetic external field. So, it can be considered as a good alternative to carry out functions of actuators or sensors in electronic or mechatronic devices.

Conclusions

A PMHM consisting of iron oxide nanoparticles into a PVB matrix was obtained. The synthesis of magnetic nanoparticles from the precursor film hybrid material or Fe(II)-PVB was confirmed via XRD and FTIR analysis. The iron-oxide nanoparticles are embedded in the PVB-matrix and their measured size was around 5 nm, having a nearly spherical morphology. The analysis of the magnetic properties of the PMHM shows a superparamagnetic behavior at room temperature changing to ferromagnetic below 25 K, the blocking temperature. Magnetorheology measurements for PMHM-sample corroborate that *G´* and tan δ can be modified by an external applied field, in other words its viscoelastic properties can be modified under action of a magnetic external field. Our results suggest that in-situ precipitation of nanoparticles in the precursor hybrid material (Fe(II)-PVB) is a promising route to the production of PMHM.

Acknowledgments

This project was financially supported by the Consejo Nacional de Ciencia y Tecnología through scholarship number 362279.

References

Abellán G., Martí-Gastaldo C., Ribera A., Coronado E. Hybrid materials based on magnetic layered double hydroxides: a molecular perspective. *Accounts of chemical research*, volume 48, 2015: 1601-1611.

Aowlad-Hossain A.B.M., Cho M.H., Lee S.Y. Magnetic nanoparticle density mapping from themagnetically induced displacement data: a simulation study. *Biomedical Engineering Online*, volume 11, 2012: 2-13.

Clark D.E. Peroxides and peroxide-forming compounds. *Chemical health & safety*, volume September/October, 2001: 12-22.

El-Din S., Nabi M., Sabaa M.W. Thermal degradation of poly (vinyl butyral) laminated safety glass. *Polymer degradation and stability*, volume 47, 1995: 283-288.

Fors C. Mechanical properties of interlayers in laminated glass. Experimental and numerical evaluation (Thesis of Master of Science), Lund University, Sweden, October 2014.

Galloway J.M., Talbot J.E., Critchley K., Miles J.J., Bramble J.B. Developing biotemplated data storage: Room temperature biomineralization of $L1_0$ CoPt magnetic nanoparticles. *Advanced functional materials*, volume 25, 2015: 4590-4600.

Gonçalves E.S., Cornejo D.R., Oliveira C.L.P., Figueiredo-Neto A.M. Magnetic and structural study of electric double-layered ferrofluid with $MnFe_2O_4$@γ-Fe_2O_3 nanoparticles of different mean diameters: determination of the magnetic correlation distance. *Physical review E.*, volume 91, 2015: 1-7.

Herbert E.G., Oliver W.C., Pharr G.M. Nanoindentation and the dynamic characterization of viscoelastic solids. *Journal of physics D: applied physics*, volume 41 (issue 7), 2008: 1-9.

ICDD. Powder Diffraction Database, Pattern No. 39-1346, 2000a.

ICDD. Powder Diffraction Database, Pattern No. 19-0629, 2000b.

Jiang F.Y., Li X.Y., Zhu Y., Tang Z.K. Synthesis and magnetic characterizations of uniform iron oxide nanoparticles. *Physica B*, volume 443, 2014: 1-5.

Joy P.A., Anil-Kumar P.S., Date S.K. The relationship between field-cooled and zero-field-cooled susceptibilities of some ordered magnetic systems. *Journal of physics: condensed matter*, volume 10, 1998: 11049-11054.

Kucheryavy P., He J., John V.T., Maharjan P., Spinu L., Goloverda G.Z., Kolesnichenko V.L. Superparamagnetic iron oxide na-

DOI: http://dx.doi.org/10.22201/fi.25940732e.2018.19n1.010

noparticles with variable size and an iron oxidation state as prospective imaging agents. *Langmuir : The ACS journal of surfaces and colloids*, volume 29 (issue 2), 2013: 710-716.

Kumar D. and Singh V. Study of heterocyclic compound tetrahydrofuran (THF). *International journal of research in science and technology*, volume 3, 2014: 29-32.

Lu A.H., Salabas E.L., Schüth F. Magnetic nanoparticles: synthesis, protection, functionalization, and application. *Angewandte chemie*, volume 46, 2007: 1222-1244.

Luna-Martínez J.F., Reyes-Melo E., González-González V., Guerrero-Salazar C., Torres-Castro A., Sepúlveda-Guzmán S. Synthesis and characterization of a magnetic hybrid material consisting of iron oxide in a carboxymethyl cellulose matrix. *Journal of applied polymer science*, volume 127 (issue 3), 2013: 2325-2331.

Marinho J.Z., Montes R.H.O., De Moura A.P., Longo E., Varela J.A., Munoz R.A.A., Lima R.C. Rapid preparation of α-FeOOH and α-Fe_2O_3 nanostructures by microwave heating and their application in electrochemical sensors. *Materials research bulletin*, volume 49, 2014: 572-576.

Philippova O., Barabanova A., Molchanov V., Khokhlov A. Magnetic polymer beads: Recent trends and developments in synthetic design and applications. *European polymer journal*, volume 47, 2011: 542-559.

Reyes-Melo E., Martínez-Vega J., Guerrero-Salazar C., Ortiz-Méndez U. On the modeling of the dynamic-elastic modulus for polymer materials under isochronal conditions. *Journal of applied polymer science*, volume 94, 2004: 657- 670.

Reyes-Melo M.E., Rentería-Baltiérrez F.Y., López-Walle B.C. Estudio de la movilidad molecular de PVB mediante análisis mecánico dinámico. *Ingenierías*, volume XVIII (issue 67), 2015: 5-11.

Shin T.H., Choi Y., Kim S., Cheon J. Recent advances in magnetic nanoparticle-based multi-modal imaging. *Chemical society review*, volume 44, 2015: 4501-4516.

Sommertune J., Sugunan A., Ahniyaz A., Stjernberg-Bejhed R., Sarwe A., Johansson Ch., Balceris Ch., Ludwig F., Posth O., Fornara A. Polymer/iron oxide nanoparticle composites—A straight forward and scalable synthesis approach. *International Journal of molecular science*, volume 16, 2015: 19752-19768.

Tan T.L., Wang L.L., Zhang J., Johnson D.D., Bai K. Platinum nanoparticle during electrochemical hydrogen evolution: Adsorbate distribution, active reaction species, and size effect. *American chemical society: catalysis*, volume 5, 2015: 2376-2383.

Teja A.S. and Koh P.Y. Synthesis, properties, and applications of magnetic iron oxide nanoparticles. *Progress in crystal growth and characterization of materials*, volume 55, 2009: 22-45.

Torres-Martínez N.E., Garza-Navarro M.A., García-Gutiérrez D., González-González V.A., Torres-Castro A., Ortiz-Méndez U. Hybrid nanostructured materials with tunable magnetic characteristics. *Journal of nanoparticles research*, volume 16 (issue 2759), 2014: 1-12.

Wu1 Y., Yang X., Yi X., Liu Y., Chen Y., Liu G., Li R.W. Magnetic nanoparticle for biomedicine applications. *Journal of Nanotechnology: Nanomedicine & Nanobiotechnology*, volume 2 (issue 003), 2015a: 1-7.

Wu1 W., Wu Z., Yu T., Jiang C., Kim W.S. Recent progress on magnetic iron oxide nanoparticles: synthesis, surface functional strategies and biomedical applications. *Science and technology of advanced materials*, volume 16, 2015b: 1-43.

Xi-Xi Q. and Zhi-Lin C. Application of ionic liquids as a catalyst in the synthesis of polyvinyl butyral (PVB) polymer. *Chinese chemical letters*, volume 27, 2016: 145-148.

Zhang Y., Zhang L., Song X., Gu X., Sun H., Fu Ch., Meng F. Synthesis of superparamagnetic iron oxide nanoparticles modified with MPEG-PEI via photochemistry as new MRI contrast agent. *Journal of nanomaterials*, 2015a: 1-6.

Zhang X., Hao H., Shi Y., Cui J. The mechanical properties of Polyvinyl Butyral (PVB) at high strain rates. *Construction and building materials*, volume 93, 2015b: 404-4015.

Zhou Z.M., David D.J., Macknight W.J., Karasz F.E. Synthesis characterization and miscibility polyvinyl butyrals of varying alcohol contents. *Tr. J. of chemistry*, volume 21, 1997: 229-238.

DOI: http://dx.doi.org/10.22201/fi.25940732e.2018.19n1.010

Suggested citation:

Chicago style citation

Reyes-Melo, Martín Edgar, Jesús Gabino Puente-Cordova, Beatriz López-Walle, Alejandro Torres-Castro, Antonio Francisco García-Loera. Synthesis and characterization of a polymeric magnetic hybrid material composed of iron oxide nanoparticles and polyvinyl butyral. *Ingeniería Investigación y Tecnología,* XIX, 01 (2018): 113-123.

ISO 690 citation style

Reyes-Melo M.E., Puente-Cordova J.G., López-Walle B., Torres-Castro A., García-Loera A.F. Synthesis and characterization of a polymeric magnetic hybrid material composed of iron oxide nanoparticles and polyvinyl butyral. *Ingeniería Investigación y Tecnología*, volume XIX (issue 1), January-March 2018: 113-123.

About the authors

Martín Edgar Reyes-Melo. Is a full professor in the Doctoral Program in Materials Science at the Universidad Autónoma de Nuevo León. He received her BS degree in Food Industry Engineer from Universidad Autónoma de Nuevo León, Mexico; her M.Sc. degree in Mechanical Engineering (Materials Science) from Universidad Autónoma de Nuevo León, México; and her PhD degree in Materials Science (Materials, Technology, and Components of Electronics) from Université Paul Sabatier (Toulouse III), Toulouse, France. Her research interests involves rheology, electric and magnetic properties of polymer systems, application of fractional calculus to modelling of polymeric hybrid materials.

Jesús Gabino Puente-Córdova. He received her BS degree in Mechanical and Electrical Engineering and her M.Sc. degree in Mechanical Engineering (Materials Science) from Universidad Autónoma de Nuevo León, Mexico. He is a Ph.D. candidate in Materials Engineering at the Universidad Autonoma de Nuevo León, México.

Beatriz López-Walle. Is an associate professor in the Doctoral Program in Materials Science at the Universidad Autónoma de Nuevo León, México. She received her BS degree in mechanical engineering from Universidad Nacional Autónoma de México, and her PhD degree in micromechatronics from Université de Franche-Comté, France. Her research interests involves study, simulation, modelling and application of smart materials (magnetic polymers and shape memory alloys) into functional micromechatronics devices.

Alejandro Torres-Castro. Is an associate professor in the Doctoral Program in Materials Science at the Universidad Autónoma de Nuevo León. He received her BS degree in Mechanical Engineering from Instituto Tecnológico de Ciudad Madero, Tamaulipas, Mexico; her M.Sc. degree in Mechanical Engineering (Materials Science) and her PhD degree in Material Engineering from Universidad Autónoma de Nuevo León. Her research interests involves, synthesis and characterization of core-shell nanoparticles.

Antonio Francisco García-Loera. Is a full professor in the Doctoral Program in Materials Science at the Universidad Autónoma de Nuevo León, México. He received her BS degree in Mechanical and Management Engineering; a Master of Science in Mechanical Engineering (Materials Science) from Universidad Autónoma de Nuevo León; a Master of Science in Materials Science at the INSA of Lyon, France; and her PhD degree in Materials Science at the INSA of Lyon, France. Her research interests involves, physicochemical of polymer blends, polymeric composite materials.

DOI: http://dx.doi.org/10.22201/fi.25940732e.2018.19n1.010